Experimental Neurology 315 (2019) 21–31

Contents lists available at ScienceDirect

Experimental Neurology

journal homepage: www.elsevier.com/locate/yexnr

Research Paper

GATA-4 regulates neuronal apoptosis after intracerebral hemorrhage via the NF-κB/Bax/Caspase-3 pathway both in vivo and in vitro

Hui Xu[a,b,1], Jie Cao[a,c,1], Jianguo Xu[a,1], Haiying Li[a], Haitao Shen[a], Xiang Li[a], Zhong Wang[a,*], Jiang Wu[a,*], Gang Chen[a]

[a] Department of Neurosurgery & Brain and Nerve Research Laboratory, The First Affiliated Hospital of Soochow University, 188 Shizi Street, Suzhou 215006, Jiangsu Province, China
[b] Department of Neurosurgery, The Sixth People's Hospital of Nantong, No. 500 Yonghe Road, Nantong 226011, Jiangsu Province, China
[c] Department of Neurosurgery, The First People's Hospital of Changzhou, Juqian Street, Changzhou 213003, Jiangsu Province, China

ARTICLE INFO

Keywords:
GATA-4
Intracerebral hemorrhage
Apoptosis
NF-κB
Bax
Caspase-3

ABSTRACT

GATA-binding protein 4 (GATA-4) , a member of the GATA family of transcription factors, is expressed in the normal brain and participates in the neural inflammatory response and senescence. However, few studies have investigated whether GATA-4 is involved in the brain damage induced by intracerebral hemorrhage (ICH). The aim of this study was to investigate in vivo and in vitro the role of GATA-4 in ICH-induced secondary brain injury (SBI) and its potential underlying mechanisms. A rat model of ICH was established by autologous blood injection in vivo. In vitro, oxidized hemoglobin was applied to mimic the effects of ICH in neuronal culture. The function of GATA-4 and its mechanism of action after ICH were investigated using siRNA-mediated knockdown and plasmid-mediated overexpression techniques combined with immunofluorescence, western blot, and other molecular methods. It was found that the expression of GATA-4 was increased in the brain of rats after ICH, and its phosphorylation also increased correspondingly. Furthermore, knocking down the expression of GATA-4 led to a significant decrease in neurobehavioral scores and neuronal apoptosis, indicating that secondary brain damage was improved. Conversely, the overexpression of GATA-4 aggravated brain damage. Blockade of a critical phosphorylation site on the GATA-4 overexpression plasmid alleviated the exacerbated damage in vitro and in vivo. Moreover, GATA-4 promoted the activation of NF-κB, and increased the expression of Bax, and cysteine aspartate-specific protease 3 (caspase-3) in its cleaved form, causing neuronal apoptosis. In conclusion, the expression of GATA-4 was increased in the brain of rats after ICH. GATA-4 phosphorylation mediates the function of the protein in ICH-induced SBI. Neuronal apoptosis after ICH was mainly induced by NF-κB activation, which was promoted by GATA-4.

1. Introduction

Intracerebral hemorrhage (ICH) is a severe cerebrovascular disease characterized by high morbidity and mortality, with an incidence rate of about 15% of all stroke cases (Song et al., 2015). Therefore, research on ICH has received increasing attention in recent years. Brain injury can be caused by damaged tissue surrounding the initial hematoma, either directly by blood clots or due to a series of pathophysiological processes following ICH such as the destruction of the blood-brain barrier, activation of apoptotic programs, and the toxic effects of extracellular heme. These pathophysiological processes are called secondary brain injury (SBI). The duration of SBI is long and the damage is often more serious than the initial ICH (Jiang et al., 2017). Therefore, our study focused on this secondary damage or SBI that occurs after ICH.

GATA-4 is an important transcription factor involved in cardiac development and plays a critical role in regulating cardiac growth and differentiation (Garg et al., 2003). In recent years, studies have reported

Abbreviations: GATA-4, GATA-binding protein 4; ICH, intracerebral hemorrhage; NF-κB, nuclear factor-kappa B; Caspase-3, cysteine aspartate-specific protease 3; SBI, secondary brain injury; SD, Sprague–Dawley; NC, negative control; EV, empty vector; siRNA, small interfering RNA; PCR, polymerase chain reaction; TUNEL, terminal deoxynucleotidyl transferase-mediated dUTP nick-end labeling; FJB, Fluoro-Jade B; BCA, bicinchoninic acid; SEM, standard error of the mean; OxyHb, oxyhemoglobin

* Corresponding authors.
E-mail address: wujiangsz@163.com (J. Wu).
[1] These authors contributed equally to this work.

https://doi.org/10.1016/j.expneurol.2019.01.018
Received 19 September 2018; Received in revised form 25 December 2018; Accepted 29 January 2019
Available online 30 January 2019

that GATA-4 induced brain inflammation and aging (Kang et al., 2015), and the expression of GATA-4 in the human brain inhibited the proliferation of astrocytes (Agnihotri et al., 2011). Some research also found that GATA-4 participated in cardiac repair after injury (Stefanovic et al., 2014; Yu et al., 2016). However, few studies have investigated the role of GATA-4 after ICH.

Previous studies have confirmed the mechanism of action of GATA-4 in some diseases; GATA-4 acts upstream of NF-κB to regulate IL6, IL8, and C-X-C motif ligand 1 (CXCL1), along with the inflammation associated with these proteins (Kang et al., 2015). GATA-4 was also shown to mediate astrocyte proliferation by regulating p21 (Cip1), which caused glioblastoma multiforme (Agnihotri et al., 2011).

In this study, we focused on the effect of GATA-4 on neuronal apoptosis and brain damage after ICH, providing a theoretical basis for SBI. A better understanding of the GATA-4 function and mechanisms after ICH may provide insight to novel therapeutic targets for the treatment of ICH injury.

2. Materials and methods

2.1. Animals and ethical approval

Nearly 200 adult male Sprague–Dawley (SD) rats weighing 300–350 g were used in this study. Adult male SD rats and pregnant rats were purchase from the Laboratory Animal Center, Medical College of Soochow University (Suzhou, Jiangsu, China). We took considerable care to reduce the number of animals used. All experiments were approved by the Ethics Committee of the First Affiliated Hospital of Soochow University, China, and followed the Animal Research: Reporting of In Vivo Experiments (ARRIVE) guidelines. All rats were housed in a quiet environment with controlled temperature and humidity.

2.2. Rat model of ICH

To perform the ICH injury, we deeply anesthetized the rats and injected autologous blood into the right basal ganglia as reported previously (Klahr et al., 2015). The site of injection was 3.5 mm lateral and 0.2 mm posterior to the bergma, at a depth of 5.5 mm from the cortical surface. The microinjector slowly infused autologous blood into the basal ganglia over the course of 5 min, and the needle was held in place for an additional 5 min after the end of the infusion (Hu et al., 2011). Bone wax was used to close the burr hole in the skull, and the skin was sutured to close the wound. Finally, the rats were returned to their cages with ad libitum access to food and water. Brain sections of the ICH-injured rats are shown in Fig. 1A. The brain was removed, and a coronal brain slice (4-mm thickness) 4 mm from the frontal pole was cut using a blade, which was fixed by 4% formamint and used for immunofluorescence staining. 3 mm front to the injection site and the perihematomal of the brain was collected and frozen in liquid nitrogen for polymerase chain reaction (PCR) and western blot.

3. Experimental design

First, 42 rats (42 of 47 rats survived the ICH surgery) were randomly and equally divided into 7 groups ($n = 6$ per group); the sham group and 6 groups at different timepoints after ICH (6 h, 12 h, 24 h, 48 h, 72 h and 7 days). At the scheduled time, rats were euthanized, and their brain tissue (from the ICH-injured hemisphere) was collected for analysis (Fig. 1B).

Next, 126 rats (126 of 142 rats survived the surgery) were randomly assigned to 7 groups (=18 rats per group): the sham group, ICH group, ICH + negative control (NC) group, ICH + GATA-4 siRNA group, ICH + the empty vector (EV) group, ICH + GATA-4 plasmid group, and ICH + GATA-4(S105A) mutant group. The ICH surgery was performed 48 h after the transfection of siRNA or plasmid in vivo. At 24 h after ICH, 6 rats from each group were euthanized and their brain tissue (from the ICH-injured hemisphere) was collected for PCR, immunofluorescent staining, Fluoro-Jade B (FJB) staining, terminal deoxynucleotidyl transferase-mediated dUTP nick-end labeling (TUNEL), and western blot assays (Fig. 1C). At 72 h after ICH, the remaining 12 rats in each group were used for neurological behavior tests.

Finally, for the in vitro experiments, cultured neurons were divided into sham and OxyHb groups. The OxyHb group was subjected to OxyHb stimulation for different time durations to mimic ICH conditions. The cultured cells were then divided into groups for the siRNA experiments and the GATA-4 mutant plasmid experiments. For the siRNA experiments, cells were divided into 6 groups: control, OxyHb, OxyHb + NC, OxyHb + GATA-4 siRNA, OxyHb + EV, and OxyHb + GATA-4 plasmid. For the GATA-4 mutant experiments, cells were divided into 5 groups: control, OxyHb, OxyHb + EV, OxyHb + GATA-4 plasmid, OxyHb + GATA-4(S105A). Neurons were transfected with siRNA or plasmid, and 48 h later, the cells were incubated for 6 h with 10 μM OxyHb to simulate ICH (Sun et al., 2018). Then, the neurons were collected for analysis by western blot and/or flow cytometry (Fig. 1D).

3.1. Reverse transcription-PCR and real-time PCR

Total RNA was extracted from brain tissue using TRIzol reagent (Invitrogen, Carlsbad, CA, USA) according to the manufacturer's instructions. Briefly, approximately 1 μL total RNA was reverse transcribed into cDNA using random primers. Then, specific primers and SYBR green I (ShineGene) fluorescent dyes were designed for real-time PCR. In real-time PCR, the fluorescence signal accumulates with increasing number of amplification cycles; therefore, the fluorescent signal intensity of SYBR Green I quantitatively represents the amount of double-stranded DNA present. The PCR protocol included 1 cycle of 94 °C for 4 min, followed by 35 cycles of 94 °C for 20 s, 60 °C for 25 s, and 72 °C for 30 s. Actin was used as the internal control. The primer sequences used in this study are listed below.

Actin, Forward 5′- CCCATCTATGAGGGTTACGC -3′ and Reverse 5′- TTTAATGTCACGCACGATTTC -3′.

GATA-4, Forward 5′- CAGAAAACGGAAGCCCAAG -3′ and Reverse 5′- GCTGCTGTGCCCATAGTGAG -3’.

3.2. Construction of the siRNAs, GATA-4 plasmid, and GATA-4 plasmid mutant

Specific siRNA against GATA-4 was obtained from Ribobio to knock down GATA-4 expression. The 3 different GATA-4 target sequences used in this study were GAGATGGGACAGGACACTA, CCACAAGATGA ATGGTATC, and GCCCAAGAATCTGAATAAA. The efficiency of all 3 siRNAs to knock down GATA-4 expression was tested, and the most efficient one (siRNA-2) was used in this study.

Specific expression plasmids for GATA-4 and GATA-4(S105A) (S105A mutant: serine 105 was substituted with alanine) were obtained from GenScript. Specifically, the target fragment was sub-cloned into a pEGFP-N2 expression vector to produce the pEGFPN2-GATA-4 construct containing the rat GATA-4 cDNA coding region (without the *E*-GFP tag). The pEGFP -N2-GATA-4 construct with the S105A mutation was also generated in the same way (without an E-GFP tag). All of the constructs were tested by DNA sequencing.

3.3. siRNA and plasmid transfection in vivo

To transfect siRNA and plasmid, Entranster in vivo RNA/DNA transfection reagent (18668–11-1 Engreen/18668-11-2 Engreen) was used during the transfection protocol as per the manufacturer's instructions. The in vivo transfection protocol introduced the siRNA or plasmid into the brain of the anesthetized rat by intracerebroventricular (i.c.v) injection, as described previously (Dang et al., 2015). Briefly, the

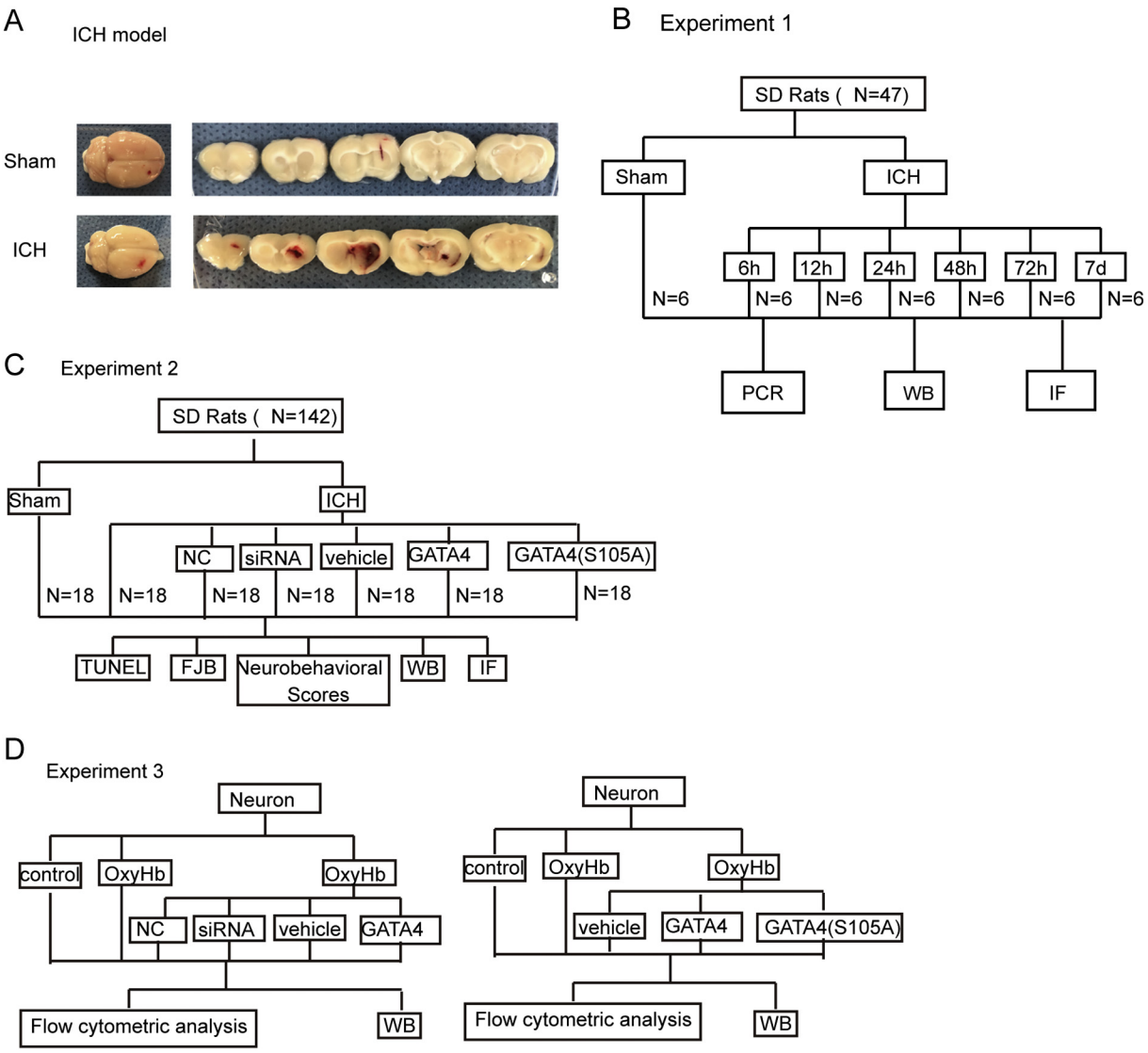

Fig. 1. Establishment of the intracerebral hemorrhage (ICH) model and experimental design.
(A) Brain slices from sham and ICH-injured rats. (B) Experimental design displaying the change of total GATA-4 and phosphorylated GATA-4 protein at different time points after ICH. (C) The effects of GATA-4 on ICH-induced secondary brain injury (SBI) in rats after the indicated interventions. (D) Experiment designed to test potential mechanisms of GATA-4 and dephosphorylation of GATA-4 after ICH.

injection site selected was in the left hemisphere, 1.0 mm lateral to the midline and 1.5 mm posterior to the bregma. The needle of the microinjector was slowly inserted into the lateral ventricle 4.0 mm below the dural surface, and the solution was infused in at a rate of about 5 μL/min.

4. Cell cultures and in vitro transfection

Cultured neurons were transfected with siRNA or plasmid using Lipofectamine 3000 Transfection Reagent (Invitrogen, Grand Island, NY) or P3000 Reagent (Invitrogen, Grand Island, NY) according to the manufacturers' instructions. Dissection and culture of primary cortical neurons from rat embryos were performed as described previously (Jiang et al., 2015). Briefly, the cortices of the rat embryos were removed cleanly and completely, then digested with 0.25% trypsin for 5 min. Next, the cortical tissue was gently pipetted up and down, and centrifuged into a suspension. Then, the neurons were added into 6-well and 12-well plates with Neurobasal Medium (GIBCO, Carlsbad, CA, USA) and incubated at 37 °C and 5% CO_2 for about 1 week (Zhai et al., 2016). When the cells reached 80% confluence, they were transfected with siRNA or plasmid and exposed to OxyHb to mimic ICH after 48 h. At the appropriate time, the neurons were harvested and stored at −80 °C until use (Kato et al., 2003).

5. Antibodies

Anti-caspase-3 antibody (ab13847), anti-Bax antibody (EPR18283, ab232479) , anti-GATA-4 antibody (EPR4768, ab134057), anti-phosphorylated GATA-4 (S105) antibodies (ab5245) and anti-NeuN antibody (1B7, ab104224) were boght from Abcam (Cambridge, MA, USA). Anti- NF-κB p65 antibody (D14E12, #8242) and anti-phosphorylated-NF-κB p65 (Ser536) antibodies (93H1, # 3033) were purchased from Cell Signaling Technology (Danvers, MA, USA). Anti-β-actin antibody (C4, sc-47778) was bought from Santa Cruz Biotechnology (Santa Cruz, CA, USA), which was used as a loading control.

5.1. Western blotting

Previously selected brain tissue samples were thoroughly lysed in an ice-cold RIPA lysis buffer (Beyotime, China) for 30 min. The lysates

were centrifuged at 12,000*g* for 10 min at 4 °C and the supernatants were collected. Protein concentration was determined using a bicinchoninic acid (BCA) assay kit (Beyotime, China). Then, protein samples (50 μg/lane for brain tissue samples and 25 μg/lane for cell culture samples) were separated on a 10% or 12% sodium dodecyl sulfate-polyacrylamide electrophoresis (SDS-PAGE) gel and electrotransferred onto a polyvinylidene fluoride (PVDF) membrane (IPVH00010, Millipore, Billerica, MA, USA). The membrane was incubated for 1 h in 5% nonfat milk at room temperature and then incubated overnight with the primary antibody at 4 °C. The next day, the membrane was incubated with the species-appropriate secondary antibody for 1 h at room temperature. Finally, the membrane was probed using the enhanced chemiluminescence (ECL) detection reagent (Clinx Science Instruments Co.), and the relative desity of the protein bands was analyzed using Image J software (National Institutes of Health, USA). β-Actin was used as a loading control.

5.2. Immunofluorescence staining

Double labeling for GATA-4 and NeuN was performed as previously described to evaluate the expression of GATA-4 in the neurons (Lan et al., 2017). Briefly, the extracted rat brain was fixed in 4% paraformaldehyde, embedded in paraffin, and then cut into 4 μm thick slices. Next, dewaxed sections were incubated with the primary antibody (anti-rabbit GATA4 antibody, 1:250; anti-mouse NeuN antibody, 1:250) overnight at 4 °C. The following day, after washing with PBST for 3 times, samples were incubated with a 1:300 dilution of the appropriate secondary antibodies (Alexa Fluor 488 donkey anti-rabbit IgG antibody, and Alexa Fluor 555 donkey anti-mouse IgG antibody; Invitrogen, Carlsbad, CA, USA). Finally, the sections were observed under a fluorescence microscope (Olympus BX50/BX-FLA/DP70, Olympus Co., Japan). To exclude the effects of exposure time and background on the result, unified exposure time was performed in an independent test, and the fluorescence intensity of the control group was normalized to 1.0. Normal rabbit IgG and normal mouse IgG were used as negative controls (data not shown). The results were analyzed by an observer who was blinded to the experimental groups. The fluorescence intensity was analyzed using the ImageJ program (NIH, Bethesda, MD, USA).

6. TUNEL staining

Using the manufacturer's protocol (In Situ Cell Death Detection Kit, Roche, Germany), TUNEL staining was performed on the brain sections to detect cellular apoptosis as described previously (Shen et al., 2015). The sections were first deparaffinized and dehydrated, followed by rehydration in xylene and a graded concentration series of ethanol. Next, the sections were incubated with the TUNEL reaction mixture for 1 h at 37 °C. After 3 washes in phosphate-buffered saline (PBS), the sections was covered with anti-quenching mounting medium containing DAPI and coverslipped. A fluorescence microscope (Olympus Co., Japan) was used to observe the TUNEL-positive neurons in each sample, and an observer blinded to the experimental groups analyzed the imaging data.

6.1. Fluoro-Jade B staining

FJB staining was performed to detect neuronal degeneration in the brain sections as described previously (Lan et al., 2017). Briefly, after being dewaxed and dehydrated, the slices were rehydrated in xylene and a graded series of ethanol, followed by permeabilization in 0.04% Triton X-100 in PBS. Next, the sections were incubated with the FJB working solution (containing 0.1% acetic acid solvent) and then incubated with a 0.06% KMnO4 solution for 15 min at room temperature. Subsequently, the sections were washed with PBS and sealed with anti-quenching mounting medium and coverslips at room temperature in a dark room. Finally, a fluorescence microscope (Olympus BX50/BXFLA/DP70, Olympus) was used for visualizing and imaging by an observer blinded to the experimental groups. The necrotic index was defined as the average number of FJB-positive cells per slice in 3 different field of view (400 ×).

6.2. Flow cytometry

An apoptosis detection kit (Kaiji Biotechnology, Nanjing, China) was used to assess neuronal apoptosis. Briefly, cultured primary neurons (after OxyHb treatment) were collected and centrifuged. The supernatant was discarded, the pellet was resuspended in the binding buffer, and 5 μL Annexin V-FITC (combined) and 5 μL propidium iodide (PI; Beyotime) were added. After incubation for 15 min at room temperature in the dark, flow cytometery was performed, and CellQuest software (BD Biosciences, New Jersey, New York, USA) was used for analysis. Apoptotic cells were quantitated by Annexin V-FITC binding and PI uptake. The cell populations positive for Annexin V-FITC and PI were considered apoptotic cells (Ye et al., 2017).

6.3. Neurological scoring

At 72 h after ICH, neurological tests were conducted on 12 rats per group to assess behavioral impairments. Behavioral performance was scored according to a previously published scoring system that monitored appetite, activity, and neurologic defects (Table 1) (Wang et al., 2015; Yamaguchi et al., 2004).

6.4. Statistical analysis

All data are expressed as the mean ± standard error of the mean (SEM). GraphPad Prism 6 was used to perform all statistical tests. One-way ANOVA was used to compare differences between multiple groups, and the independent Student's *t*-test was used to analyze the differences between 2 groups. Neurobehavioral scoring is presented as the median with the interquartile range. $P < .05$ was considered to be a statistically significant difference.

Sample sizes ($n = 6$) for animal studies were determined by power calculations for the primary parameter with mean differences and standard deviations based on pilot studies or the literature ($\alpha = 0.05$, power > 0.75).

7. Results

7.1. The level of GATA-4 was elevated after ICH

After inducing the ICH injury in rats, we determined the level of GATA-4 mRNA in the brain with real-time PCR at different time points post-ICH. The results showed that the level of GATA-4 mRNA increased significantly from 6 h after ICH compared with the sham group and reached a peak at 24 h post-injury. Across the longer time spans (48 h and 72 h), we observed that GATA-4 mRNA decreased gradually and was similar to the sham group 7 days post-ICH (Fig. 2A). We

Table 1
Scoring system for neurobehavioral testing.

	Behavior	Score
Appetite	Finished meal	0
	Left meal unfinished	1
	Scarcely ate	2
Activity	Walk and reach at least 3 corners of the cage	0
	Walk with some stimulation	1
	Almost always lying down	2
Deficits	No deficits	0
	Unstable walk	1
	Unable to walk	2

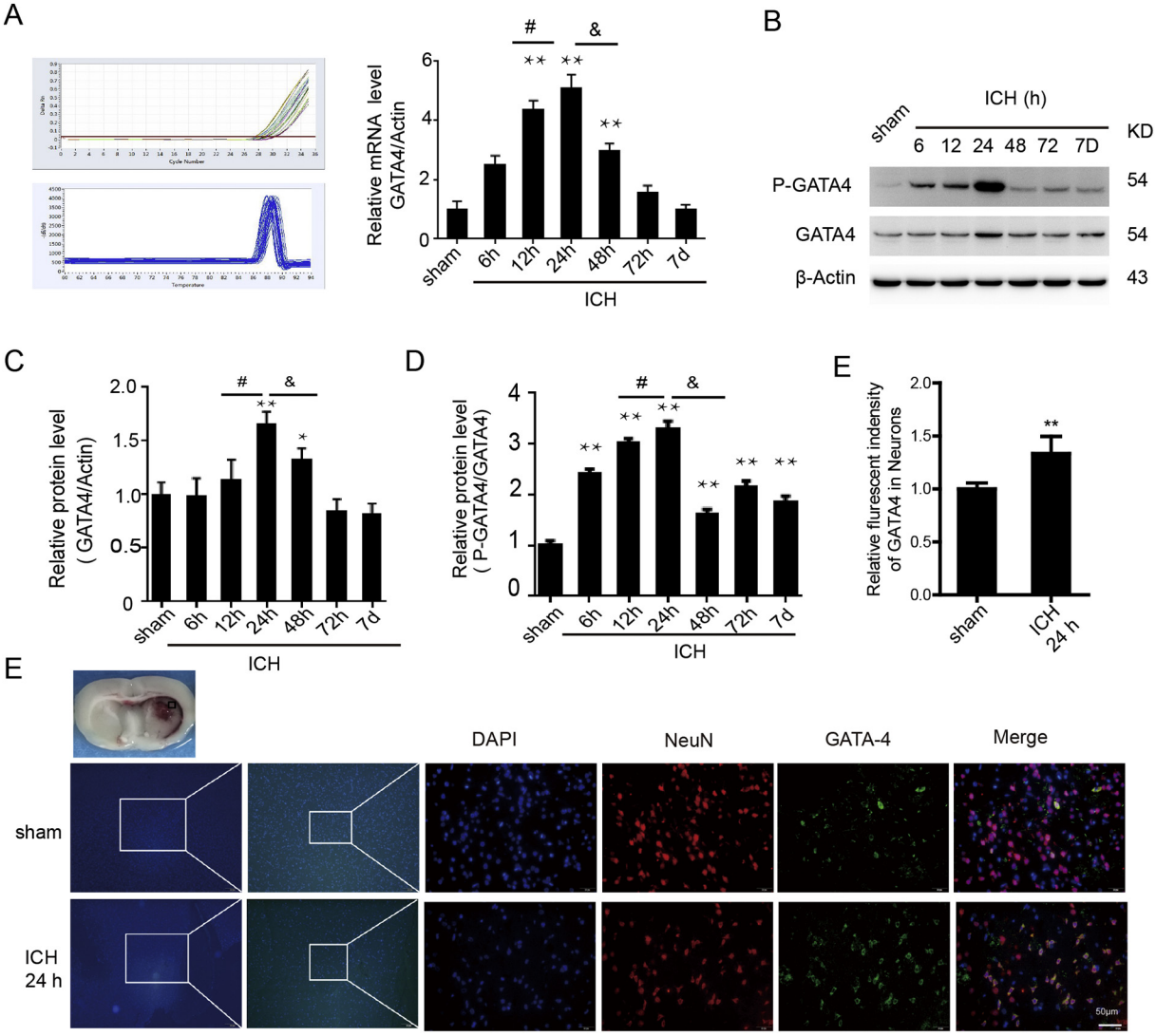

Fig. 2. Protein and mRNA levels of GATA-4 were increased in the rat brain after ICH.
(A) GATA-4 mRNA expression level at different times after ICH. Relative mRNA levels (GATA-4/β-Actin) were quantified, and all values are expressed as the mean ± SEM $^{**}P < .001$ vs. sham, $^{\#}P < .001$ for 12 h vs. 24 h, $^{\&}P < .001$ for 24 h vs. 48 h, $n = 6$. (B) Protein levels of total GATA-4 and phosphorylated GATA-4 assayed by western blot. (C, D) Quantification of the GATA-4 protein, where the relative protein levels in the sham group were normalized to 1.0 and β-Actin served as the loading control. All values are expressed as the mean ± SEM. $^{*}P < .005$ and $^{**}P < .001$ vs. sham, $^{\#}P < .001$ for 12 h vs. 24 h, $^{\&}P < .001$ for 24 h vs. 48 h, n = 6. (E) Immunofluorescent staining of brain sections from the sham and ICH groups with anti-GATA-4 antibody (green), anti-NeuN antibody (red), and DAPI (blue). Scale bar = 50 μm. (For interpretation of the references to colour in this figure legend, the reader is referred to the web version of this article.)

simultaneously examined the protein levels of GATA-4 by western blotting rat brain tissue at different time points after ICH. The results revealed a trend of GATA-4 protein expression similar to the GATA-4 mRNA expression, increasing starting at the 12 h time point after ICH compared with the sham group, reaching a high-point at 24 h, and then decreasing. The phosphorylation levels of the GATA-4 protein were also assessed; phosphorylated GATA-4 expression was similarly elevated with the total GATA-4, reaching its peak at 24 h after ICH (Fig. 2B-D). Also, it was demonstrated that phosphorylation of GATA-4 developed earlier than upregulation of GATA-4 mRNA expression (Fig. 2C and D). Consistent with the GATA-4 protein expression, immunofluorescent staining in vivo further confirmed that the GATA-4 protein was expressed in neurons and also increased after ICH (Fig. 2E).

7.2. GATA-4 induced brain damage in ICH-injured rats

To clarify the effect of the expression changes in GATA-4 following ICH on the rat brain, we transfected animals with siRNA and plasmids specific to GATA-4 and performed western blots, neurobehavioral tests, and FJB staining. Some studies indicated that the mechanism of the GATA-4 function involved Serine 105 phosphorylation (van Berlo et al., 2011), so we also designed an S105A mutation in GATA-4 that would prevent its phosphorylation at amino acid 105. The post-ICH increase in endogenous GATA-4 was decreased significantly when ICH-injured rats were transfected with GATA-4 siRNA compared with the NC group. After transfection with the GATA-4 plasmids or S105A mutant plasmid, the GATA-4 protein levels were significantly overexpressed compared with the EV group (Fig. 3A and B).

The neurological behavior of rats was severely impaired after ICH compared with the sham group. Transfection with GATA-4 siRNA significantly relieved this neurobehavioral deficit. In contrast, the same deficits were more pronounced in the ICH-injured rats transfected with the GATA-4 plasmid than in just ICH-injured rats. Notably, the impairment of neurological behaviors in the ICH + GATA-4(S105A) group was significantly less apparent than in the ICH + GATA-4 plasmid group (Fig. 3C). FJB staining showed increased degeneration in the

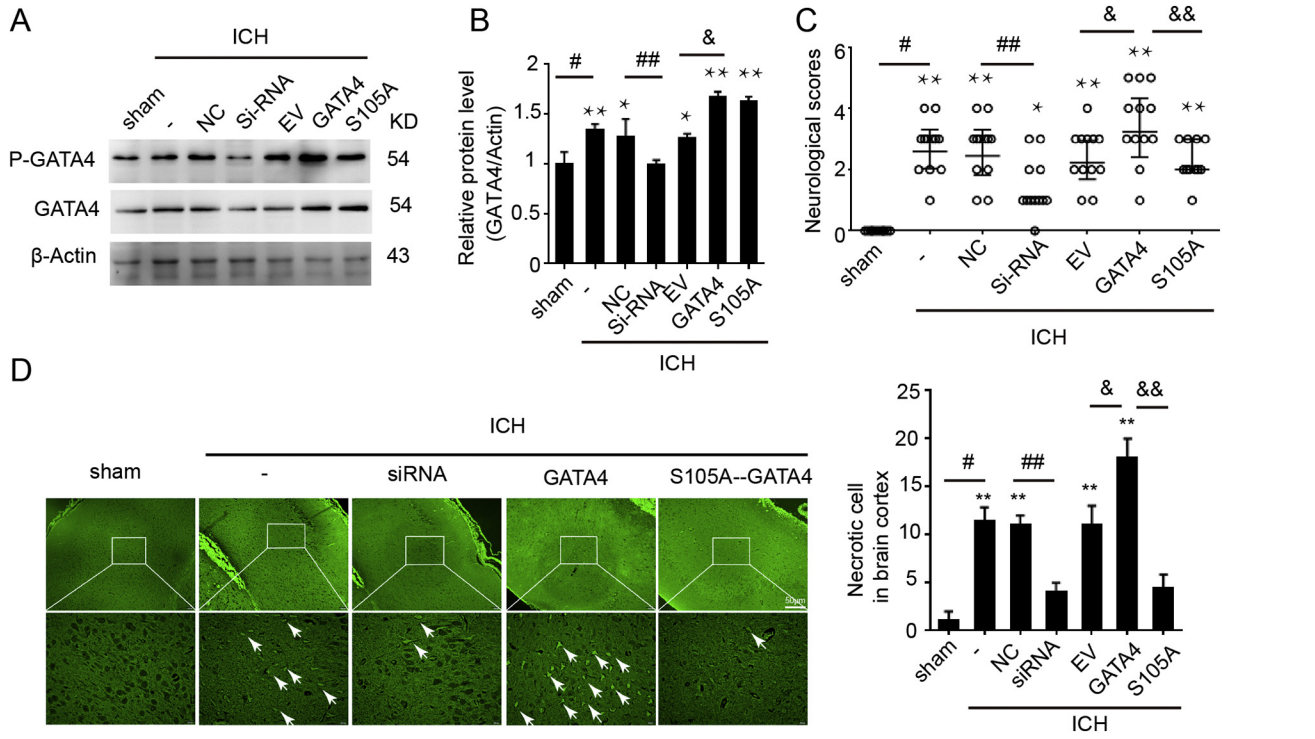

Fig. 3. GATA-4 protein induced brain damage in ICH injured rats.
(A, B) Protein levels of total GATA-4 and phosphorylated GATA-4 in the rat brain were detected by western blot after the indicated interventions. The relative protein level of GATA-4 was quantified (with β-Actin as the loading control), and the mean value in the sham group was normalized to 1.0. Data are expressed as the mean ± SEM. $^{*}P < .005$ and $^{**}P < .001$ vs. sham, $^{\#}P < .001$ for sham vs. ICH, $^{\#\#}P < .001$ for ICH + the Negative Control (NC) vs. ICH + GATA-4 siRNA, $^{\&}P < .001$ for ICH + the Empty Vector (EV) vs. ICH + GATA-4 plasmid, n = 6. (C) Neurological scores were evaluated as indicated in Table 1. $^{*}P < .005$, and $^{**}P < .001$ vs. sham; $^{\#}P < .001$ for sham vs. ICH, $^{\#\#}P < .005$ for ICH + NC vs. ICH + gata-4 siRNA, $^{\&}P < .005$ for ICH + EV vs. ICH + GATA-4 plasmid, $^{\&\&}P < .005$ for ICH + GATA-4 plasmid vs. ICH + GATA-4(S105A) mutant plasmid. $n = 12$. (D) Neuronal degradation after ICH measured by Fluoro-Jade B (FJB) staining in the cerebral cortex, quantified as FJB-positive cells/mm^2. Arrows point to FJB-positive cells. Scale bar = 50 μm. $^{**}P < .001$ vs. sham, $^{\#}P < .001$ for sham vs. ICH, $^{\#\#}P < .001$ for ICH + NC vs. ICH + GATA-4 siRNA, $^{\&}P < .001$ for ICH + EV vs. ICH + GATA-4 plasmid, $^{\&\&}P < .001$ for ICH + GATA-4 plasmid vs. ICH + GATA-4(S105A) mutant plasmid, n = 6.

brain after ICH. This degeneration was significantly reduced after siRNA transfection and approached the level of the sham group. In contrast, degeneration of the GATA-4 plasmid overexpression group was significantly increased and statistically different from that of the sham group. In the GATA-4 (S105A) mutant group, degeneration was significantly reduced and was comparable to that of the GATA group (Fig. 3D).

7.3. GATA-4 induced neuronal apoptosis in vivo

Apoptosis of neurons was also detected by TUNEL staining. Similar to the trend shown by FJB, TUNEL revealed significantly increased apoptosis in neurons after ICH. In the siRNA group, neuronal apoptosis was reduced, whereas GATA-4 overexpression (GATA-4 plasmid group) led to significantly increased apoptosis. The S105A mutation in GATA-4 caused neuronal apoptosis to decrease significantly to levels similar to those of the siRNA group (Fig. 4A and B). To further investigate the effect of the GATA-4 protein on apoptosis, we examined caspase-3. Western blot analysis showed that the protein level of cleaved caspase-3 was significantly increased in the ICH group compares with the sham group. After treatment with siRNA and the GATA-4 plasmid, caspase-3 activation was reduced and increased, respectively, tracing the expression changes of GATA-4 protein. However, in the S105A phosphorylation mutant of GATA-4, the cleaved caspase-3 expression was decreased, contrary to the increase in the caspase-3 upon GATA-4 overexpression (Fig. 4C and D). Bax protein levels, consistent with the expression pattern of caspase-3, were significantly increased in the ICH group, reduced in the siRNA group, and increased in the GATA-4 overexpression group. Similarly, in S105A mutant group, Bax protein levels were reduced (Fig. 4E and F).

7.4. GATA-4 induced neuronal cell apoptosis in vitro

We cultured primary rat neurons and treated them with OxyHb to mimic ICH. Western blot analysis showed that GATA-4 protein expression was highest in the 6 h group (Fig. 5A and B). Neurons were also treated with OxyHb and transfected with siRNA and plasmid at the indicated doses for 6 h. We first analyzed the level of knockdown and overexpression of GATA-4 on neurons by western blot. Our data indicated that the GATA-4 protein was induced in neurons under OxyHb treatment, and appropriately reduced and increased in the siRNA knockdown and overexpression group, respectively (Fig. 5C and D). Next, we compared the GATA-4 plasmid group with the GATA-4(S105A) mutant plasmid group. Western blot results showed that the expression of GATA-4 was increased in both the plasmid group and mutated plasmid group after the OxyHb treatment. The expression of phosphorylated GATA-4 was increased significantly in the plasmid group and increased slightly in the mutant plasmid group, similar to the OxyHb group (Fig. 5E-G). Finally, we tested neuronal apoptosis in vitro to understand the relationship between the GATA-4 expression and cell death. Apoptotic neurons were labeled with Annexin V-FITC and PI and analyzed by flow cytometry, early-stage apoptotic cells were increased after the OxyHb treatment, decreased in cells with the GATA-4 siRNA knockdown, and significantly increased again in cells overexpressing the GATA-4 plasmid. However, cells transfected with GATA-4(S105A) showed a significantly reduced number of apoptotic neurons (Fig. 5H).

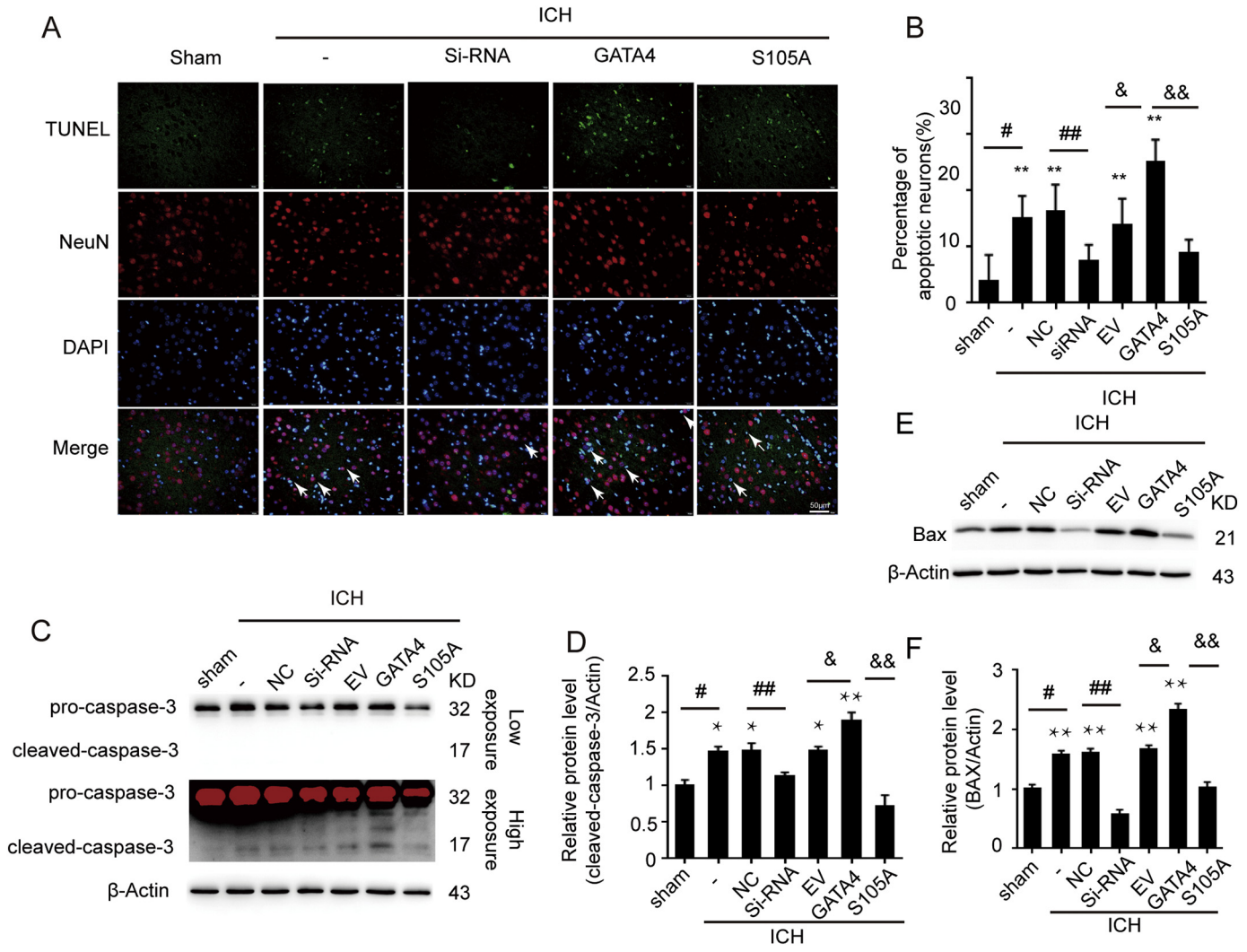

Fig. 4. GATA-4 protein led to neuronal apoptosis in vivo.
(A, B) TUNEL staining shows TUNEL (green), NeuN (red), and nuclei labeled with DAPI (blue). Arrows pointe to apoptosis-positive neurons. Scale bar = 50 μm. The percentage of apoptotic neurons was quantified, and data are expressed as the mean ± SEM, $^{**}P < .001$ vs. sham, $^{\#}P < .001$ for sham vs. ICH, $^{\#\#}P < .001$ for ICH + NC vs. ICH + GATA-4 siRNA, $^{\&}P < .001$ for ICH + EV vs. ICH + GATA-4 plasmid, $^{\&\&}P < .001$ for ICH + GATA-4 plasmid vs. ICH + GATA-4(S105A) mutant plasmid, $n = 6$. (C, D) Protein levels of cleaved-caspase-3 detected by western blot. The relative protein levels were quantified with β-Actin as the loading control. Data are expressed as the mean ± SEM, where the mean value of the sham group was normalized to 1.0. $^{*}P < .005$ and $^{**}P < .001$ vs. sham, $^{\#}P < .001$ for sham vs. ICH, $^{\#\#}P < .001$ for ICH + NC vs. ICH + GATA-4 siRNA, $^{\&}P < .001$ for ICH + EV vs. ICH + GATA-4 plasmid, $^{\&\&}P < .001$ for ICH + GATA-4 plasmid vs. ICH + GATA-4 (S105A) mutant plasmid, n = 6. (E, F) Bax protein expression data are presented as the mean ± SEM. β-Actin served as the loading control, and the mean value of the sham group was normalized to 1.0. $^{**}P < .001$ vs. sham, $^{\#}P < .001$ for sham vs. ICH, $^{\#\#}P < .001$ for ICH + NC vs. ICH + GATA-4 siRNA, $^{\&}P < .001$ for ICH + EV vs. ICH + GATA-4 plasmid, $^{\&\&}P < .001$ for ICH + GATA-4 plasmid vs. ICH + GATA-4 (S105A) mutant plasmid, n = 6. (For interpretation of the references to colour in this figure legend, the reader is referred to the web version of this article.)

7.5. GATA-4 induced neuronal cell death via the GATA-4/NF-κB/Bax/caspase-3 signaling pathway

In order to investigate the underlying molecular mechanisms of GATA-4 after ICH, we first analyzed the effects of the knockdown and overexpression of GATA-4 on neurons. GATA-4 has been shown to regulate the function of NF-κB (Kang et al., 2015), so we western blotted neurons for p65 (total protein and Ser 536-phosphorylated protein), a member of the NF-κB protein family. The data demonstrated that the phosphorylation of p65 was decreased in GATA-4 siRNA group and was increased by the overexpression of GATA-4, but the level of total p65 was not changed significantly in either group (Fig. 6A and B). Some studies suggested that p65 can induce apoptosis (Zhang et al., 2014), so we also tested the expression level of Bax and caspase-3 by western blot. The data indicated that the expression of Bax was significantly decreased by the knockdown of GATA-4 and increased by the overexpression of GATA-4 (Fig. 6C and D). Caspase-3 and cleaved caspase-3, which are critical apoptotic proteins, were induced in neurons after OxyHb treatment. In addition, the expression of cleaved caspase-3 changed corresponding to the expression of the GATA-4 protein; it reduced and increased in the GATA-4 knockdown and overexpression condition, respectively (Fig. 6E and F).

8. The effects of GATA-4 on neurons depends on its phosphorylation

In this study, we found that neuronal apoptosis was reduced when cells contained the S105A mutant of GATA-4, so we hypothesized that a possible mechanism of GATA-4-induced apoptosis was that the phosphorylation of GATA-4 could lead to an increase in p65 phosphorylation, leading to apoptosis. Western blots of phosphorylated p65 (p-p65) in cells transfected with the GATA-4 plasmid or the GATA-4 S105A

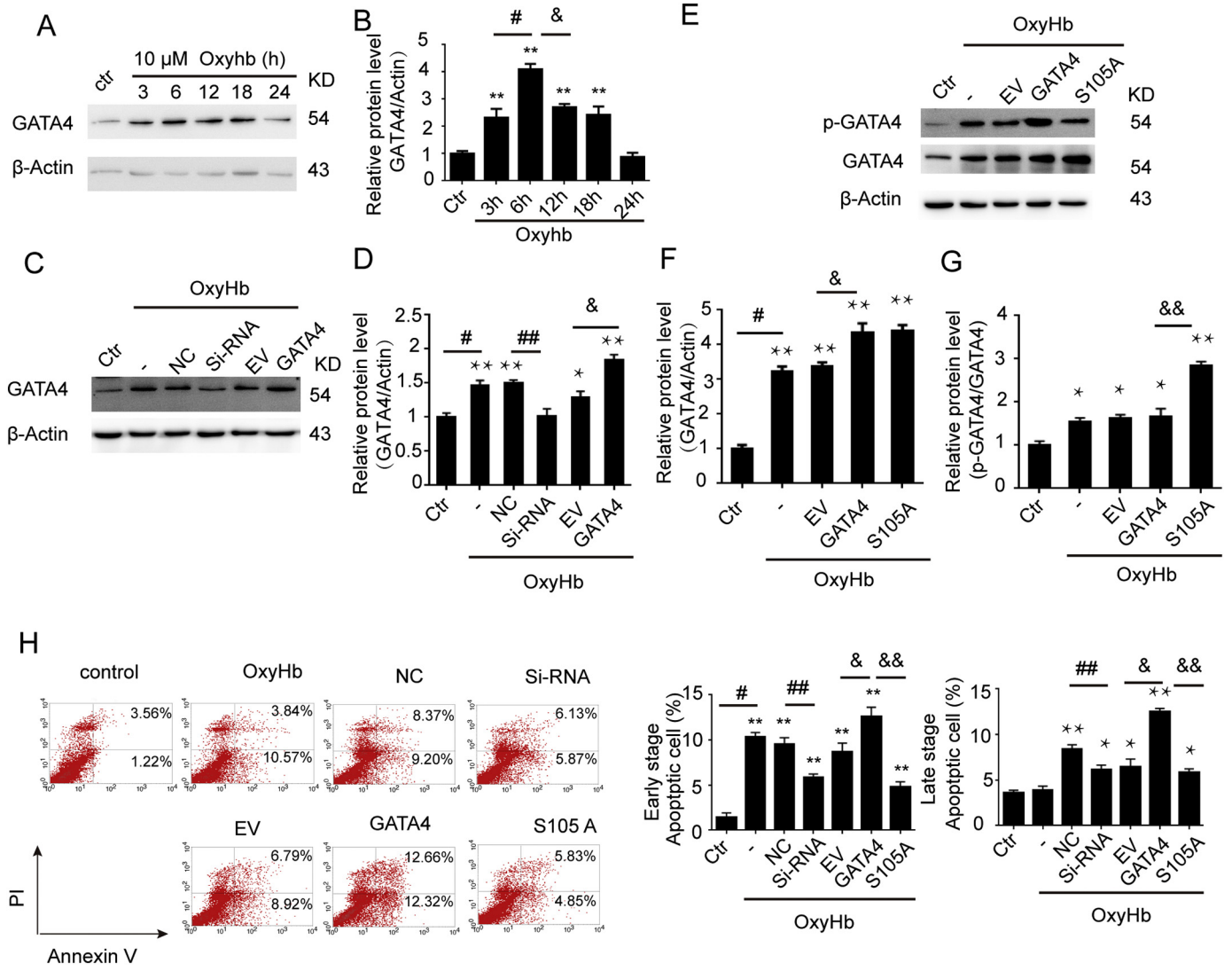

Fig. 5. GATA-4 induced apoptosis in cultured primary neurons in vitro.
(A, B) Neurons were stimulated with 10 μM OxyHb for different time durations, and the GATA-4 protein levels were detected by western blot and quantified. β-Actin served as the loading control. Data are expressed as the mean ± SEM, where the mean value of the control group was normalized to 1.0. $^{**}P < .001$ vs. control, $^{\#}P < .001$ for 3 h vs. 6 h, $^{\&}P < .001$ for 6 h vs. 12 h, $n = 3$. (C, D) Neurons were transfected with siRNA or plasmid, and cells were collected for western blot to detect the protein levels of GATA-4. Relative GATA-4 protein levels were quantified, and the mean values in the control group were normalized to 1.0. β-Actin served as the loading control. Data are expressed as the mean ± SEM $^{*}P < .005$; and $^{**}P < .001$ vs. control, $^{\#}P < .001$ for Control vs. OxyHb, $^{\#\#}P < .001$ for NC vs. GATA-4 siRNA, $^{\&}P < .001$ for EV vs. GATA-4 plasmid, $n = 3$. (E, F, G) Neurons transfected with GATA-4 plasmid or GATA-4 (S105A) mutant plasmid were collected for western blot to detect the protein levels of GATA-4 and p-GATA-4. The mean values of GATA-4/β-Actin (F) and p-GATA-4/total GATA-4 (G) in the control group were normalized to 1.0. All data are expressed as the mean ± SEM. $^{*}P < .005$; and $^{**}P < .001$ vs. control; $^{\#}P < .001$ for Control vs. OxyHb, $^{\&}P < .001$ for EV vs. GATA-4 plasmid, $^{\&\&}P < .001$ for GATA-4 plasmid vs. GATA-4 (S105A) mutant plasmid. (H) Neurons were transfected with siRNA, plasmid, or mutant plasmid and then stimulated with OxyHb. Apoptotic neurons were detected by flow cytometry and are presented as an index of the early and late stages of apoptosis. $^{*}P < .005$ and $^{**}P < .001$ vs. control, $^{\#}P < .001$ for Control vs. OxyHb, $^{\#\#}P < .001$ for NC vs. GATA-4 siRNA, $^{\&}P < .001$ for EV vs. GATA-4 plasmid, $^{\&\&}P < .001$ for GATA-4 plasmid vs. GATA-4 (S105A) mutant plasmid, n = 3.

mutant plasmid showed that the level of p-p65 was increased after the OxyHb treatment and further increased visibly in the GATA-4 overexpression group. Consistent with our hypothesis, phosphorylation-deficient GATA-4 (S105A mutant) correspondingly reduced the level of p65 phosphorylation (Fig. 7A and B). The protein levels of Bax were increased significantly in the GATA-4 overexpression group compared to the control and increased slightly in the GATA-4(S105A) mutant group (Fig. 7C and D). The protein levels of cleaved caspase-3 were similar to the trend of expression of p-p65 and Bax (Figs. 7E and F).

9. Discussion

ICH often cause residual limb dysfunction or death and has attracted increasing attention over the years. The primary brain injury after ICH is caused at the moment of its occurrence, while the secondary brain injury occurs later, lasts longer, and has more severe consequences. Therefore, the current treatment of ICH is focused on the prevention and treatment of SBI. Despite the novel results reported in our study, there is still an urgent need to study the mechanisms of SBI in depth to find new targets for the treatment of ICH.

GATA-4 is a transcription factor that is important for cardiac development. It was confirmed that GATA-4 plays a critical role in regulating cardiac development and differentiation, and genetic variations in GATA-4 are closely related to the occurrence of congenital heart disease. Previous research has shown that GATA-4 is mainly expressed in the heart, intestinal epithelium, primitive endoderm, and gonads

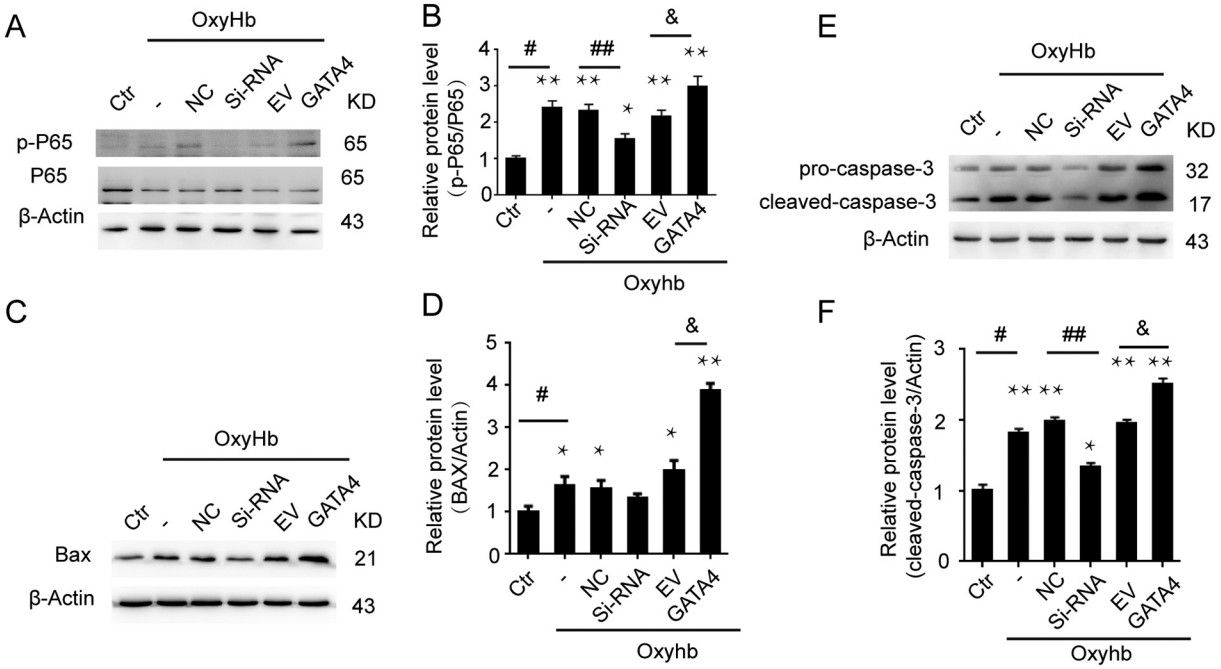

Fig. 6. NF-κB, Bax, and caspase-3 levels changed corresponding to changes in GATA-4.
Neurons were transfected with siRNA or plasmid and then stimulated with OxyHb. The cells were collected and prepared for western blotting. (A, B) Protein levels of phosphorylated p65 (p-p65) and total p65 are presented as p-p65/p65 with the control group normalized to 1.0. β-Actin served as the loading control. Data are expressed as the mean ± SEM. $^{*}P < .005$ and $^{**}P < .001$ vs. Control, $^{\#}P < .001$ for Control vs. OxyHb, $^{\#\#}P < .001$ for NC vs. GATA-4 siRNA, $^{\&}P < .001$ for EV vs. GATA-4 plasmid, n = 3. (C, D) Protein levels of Bax are presented as relative mean values of Bax/β-Actin, with the control group normalized to 1.0. β-Actin served as the loading control. All data are expressed as the mean ± SEM. $^{*}P < .005$ and $^{**}P < .001$ vs. control, $^{\#}P < .001$ for Control vs. OxyHb, $^{\&}P < .001$ for EV vs. GATA-4 plasmid, n = 3. (E, F) Protein levels of cleaved-caspase-3 are present as the relative density of cleaved-caspase-3/total caspase-3, with the control group normalized to 1.0. β-Actin served as the loading control. Data are expressed as the means ± SEM. $^{*}P < .005$ and $^{**}P < .001$ vs. Control, $^{\#}P < .001$ for Control vs. OxyHb, $^{\#\#}P < .001$ for NC vs. GATA-4 siRNA, $^{\&}P < .001$ for EV vs. GATA-4 plasmid, n = 3.

(Arceci et al., 1993). In recent studies, it has been found that damaged rat embryonic fibroblasts induced an inflammatory response and senescence by inhibiting the autophagy of GATA-4 (Kang et al., 2015) and that GATA-4 expression in the human brain inhibited the proliferation of astrocytes (Agnihotri et al., 2011). Adding to the body of knowledge regarding the role of GATA-4 in the brain, our experiments showed that the expression of GATA-4 was increased after ICH. The phosphorylation of GATA-4 developed earlier than upregulation of GATA-4 mRNA expression. GATA4 can be directly phosphorylated or dephosphorylated to facilitate inducible hypertrophic gene expression. And it has been demonstrated that phosphorylation of GATA4 at S105 is critical for a productive cardiac hypertrophic response to stress stimulation in adult mice (van Berlo et al., 2011). As a response to stress for phosphorylation of GATA4, it could be the reason why it developed earlier.

A large number of studies have provided evidence of apoptosis in tissues surrounding the hematoma after a cerebral hemorrhage (Bobinger et al., 2017). In addition, our own previous investigations showed that the expression of GATA-4 increased in neurons after ICH. Therefore, we hypothesized that GATA-4 could mediate some of the neuronal changes that take place after ICH such as apoptosis or neuroprotection. The results of our study indicated that neuronal apoptosis was altered corresponding to the increase or decrease in GATA-4 expression, suggesting that GATA-4 played a role in neuronal apoptosis after ICH. In our study, we found that cleaved caspase-3 changed proportionally with GATA-4 in ICH-injured rats in vitro and in vivo. These findings clarified that GATA-4 was involved in caspase-3-dependent neuronal apoptosis after ICH. In addition, apoptosis can be induced either by the mitochondria-mediated intrinsic pathway or the death receptor-mediated extrinsic signaling pathway (Burz et al., 2009). Bax, the Bcl-2 family member and pro-apoptotic protein, is essential for maintaining the integrity of the mitochondrial membrane. In our study, an obvious increase of cleaved caspase-3 was observed in the brain tissue after ICH, which changed alongside the level of the GATA-4 protein. We also found that the expression of the intrinsic pathway-associated protein, Bax, increased or decreased with the corresponding change in the GATA-4 levels. Taken together, these findings support the mechanism that GATA-4 regulates neuronal apoptosis after ICH via the intrinsic pathway.

Furthermore, Some studies reported an increase in the NF-κB activity under pathological conditions that cause neuron death (Clemens et al., 1997; Grilli et al., 1996). A previous report suggested that GATA-4 depletion inhibited NF-κB activation, implying that GATA-4 can promote the activation of NF-κB (Kang et al., 2015). These findings were similar to our experimental results; when the expression of GATA-4 was increased or decreased, we observed a corresponding change in the expression of the NF-κB family member p65. Taken together, these findings suggest that GATA-4 functions upstream of NF-κB and plays a role in its activation.

Studies have shown that the GATA-4 function is regulated by its phosphorylation at serine 105 (van Berlo et al., 2011). In order to understand how GATA-4 activates NF-κB and induces apoptosis, we focused on this phosphorylation event of GATA-4. In our study, we found that the GATA-4 protein regulated NF-κB in a phosphorylation-dependent manner, p65 phosphorylation, a feature for NF-κB activation was increased when GATA-4 was overexpressed, but the S105A mutation that prevented GATA-4 phosphorylation caused p65 phosphorylation to be reduced significantly. It is important to note that the S105A mutation did not reduce the expression of total GATA-4 protein or mute the function of the endogenous protein in any other way. Our findings indicated that GATA-4 activated downstream proteins while in its phosphorylated state. And GATA-4 was phosphorylated at Ser 105 amino acid site during ICH, which could activate NF-κB signaling pathway and induce mitochondrial mediate neuronal cell apoptosis. However, in this research, we only study the phosphorylation of GATA-4 at S105,

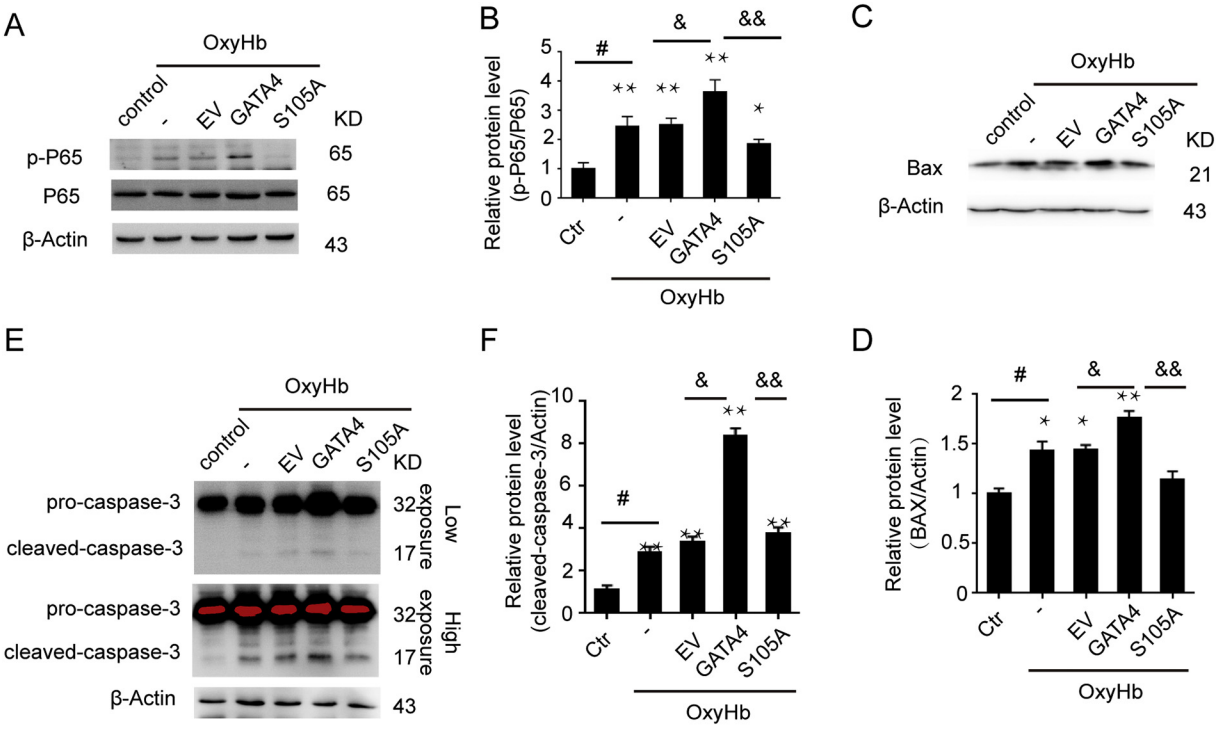

Fig. 7. The role of GATA-4 depends on its phosphorylation state.
Neurons were transfected with GATA-4 plasmid or mutant plasmid and then stimulated with OxyHb. The cells were collected and prepared for western blotting. (A, B) p-p65 and p65 protein levels after transfection with GATA-4 plasmid or mutant plasmid in vitro. The relative data of p-p65/p65 in the control group were normalized to 1.0. β-Actin served as the loading control. Data are expressed as the mean ± SEM. $^{*}P < .005$, and $^{**}P < .001$ vs. control, $^{\#}P < .001$ for Control vs. OxyHb; $^{\&}P < .001$ for EV vs. GATA-4 plasmid, $^{\&\&}P < .001$ for GATA-4 plasmid vs. GATA-4(S105A) mutant plasmid, n = 3. (C, D) Western blots showing the relative protein level of Bax after the indicated interventions in vitro. The mean values (Bax/β-Actin) in the control group were normalized to 1.0. β-Actin served as the loading control. Data are expressed as the mean ± SEM. $^{*}P < .005$ and $^{**}P < .001$ vs. control, $^{\#}P < .001$ for Control vs. OxyHb, $^{\&}P < .001$ for EV vs. GATA-4 plasmid; $^{\&\&}P < .001$ for GATA-4 plasmid vs. GATA-4 (S105A) mutant plasmid, n = 3. (E, F) Relative protein level of cleaved caspase-3, with mean values (cleaved-caspase-3/total caspase-3) in the control group normalized to 1.0. β-Actin served as the loading control. Data are expressed as the mean ± SEM. $^{*}P < .005$, and $^{**}P < .001$ vs. control, $^{\#}P < .001$ for Control vs. OxyHb, $^{\&}P < .001$ for the EV vs. GATA-4 plasmid, $^{\&\&}P < .001$ for GATA-4 plasmid vs. GATA-4 (S105A) mutant plasmid, n = 3.

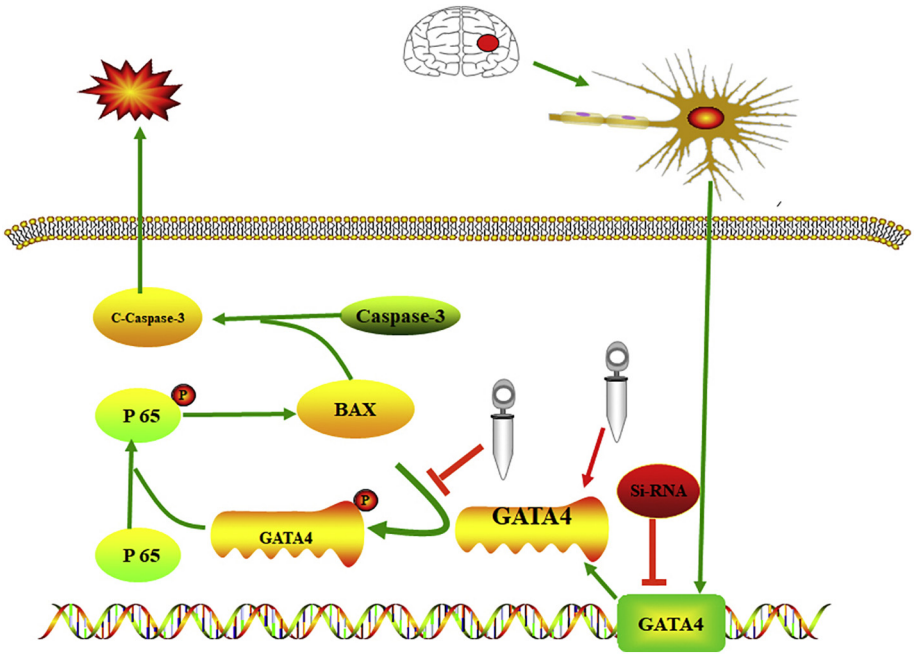

Fig. 8. The mechanism of GATA-4 in SBI after ICH.
After ICH onset, the expression of the GATA-4 protein is increased. The function of GATA-4 gets enhanced by phosphorylation and activates p65 to form phosphorylated p65. Next, p-p65 activates Bax, followed by cleaved caspase-3, inducing neuronal apoptosis and behavioral deficits in rats. The green arrows indicate the effects after ICH and the red arrows indicate the effects of the experimental interventions. (For interpretation of the references to colour in this figure legend, the reader is referred to the web version of this article.)

whether the phosphorylation at other sites of GATA-4 also played a similar role, and what was the regulation of phosphorylation need to be further researched.

In addition, GATA-4, as an upstream of NF-κB, also regulates senesce-associated secretory phenotype (SASP), a pro-inflammatory response (Kang et al., 2015). Also, GATA4 could regulate inflammation in rheumatoid arthritis (Jia et al., 2018). As a result of inflammation, breakdown of the blood-brain barrier (BBB) takes place during SBI after ICH. As well, this progress could contribute to inflammation by promoting leucocyte infiltration. Based on the reported research, I supposed that GATA4 may participate in BBB disruption though induction of inflammation after ICH, which would be further researched.

We acknowledge that our study has its limitations. In order to minimize the variables involved, we used only adult male rats for all the ICH experiment, but it clinically occurs mostly in the elderly. Future experiments should investigate ICH in aged rats to better simulate the human condition. Moreover, in order to investigate a potential mechanism of hemorrhagic damage in this experiment, infusing autologous whole blood was used to create the blood model, which was thought to mimic the large bleed similar to the most ICH patients. However, there are still some disadvantages in this model, such as it cannot mimic the ICH in human perfectly. Although there is similar functional impairment at the beginning, the recovery of neurological deficit is rapid and complete, which is inconsistent with the persistent and debilitating deficits seen in ICH patients, and it is difficult to assess long-term outcome accurately (MacLellan et al., 2008).

10. Conclusion

In conclusion, our work provided a new perspective on the cellular mechanisms of neuronal apoptosis after ICH. The ICH induced an increase in the expression of the GATA-4 protein, which resulted in an increase in neuronal apoptosis (Fig. 8). Thus, GATA-4 could be a potential therapeutic target for the treatment of ICH-induced brain injury.

Acknowledgements

This work was supported by the Project of Jiangsu Provincial Medical Innovation Team (No. CXTDA2017003), Suzhou Key Medical Centre (No. Szzx201501), Scientific Department of Jiangsu Province (No. BE2017656), Suzhou Government (No. LCZX201601), the National Natural Science Foundation of China (No. 81701210), and the National Key R&D Program of China (No. 2018YFC1312600 & No. 2018YFC1312601).

Conflicts of interest

The authors declare that there are no conflicts of interest.

References

Agnihotri, S., Wolf, A., Munoz, D.M., Smith, C.J., Gajadhar, A., Restrepo, A., Clarke, I.D., Fuller, G.N., Kesari, S., Dirks, P.B., McGlade, C.J., Stanford, W.L., Aldape, K., Mischel, P.S., Hawkins, C., Guha, A., 2011. A GATA4-regulated tumor suppressor network represses formation of malignant human astrocytomas. J. Exp. Med. 208, 689–702.

Arceci, R.J., King, A.A., Simon, M.C., Orkin, S.H., Wilson, D.B., 1993. Mouse GATA-4: a retinoic acid-inducible GATA-binding transcription factor expressed in endodermally derived tissues and heart. Mol. Cell. Biol. 13, 2235–2246.

van Berlo, J.H., Elrod, J.W., Aronow, B.J., Pu, W.T., Molkentin, J.D., 2011. Serine 105 phosphorylation of transcription factor GATA4 is necessary for stress-induced cardiac hypertrophy in vivo. Proc. Natl. Acad. Sci. U. S. A. 108, 12331–12336.

Bobinger, T., Burkardt, P., Huttner, H.B., Manaenko, A., 2018. Programmed cell death after intracerebral hemorrhage. Curr. Neuropharmacol. 16, 1267–1281.

Burz, C., Berindan-Neagoe, I., Balacescu, O., Irimie, A., 2009. Apoptosis in cancer: key molecular signaling pathways and therapy targets. Acta Oncol. 48, 811–821.

Clemens, J.A., Stephenson, D.T., Smalstig, E.B., Dixon, E.P., Little, S.P., 1997. Global ischemia activates nuclear factor-kappa B in forebrain neurons of rats. Stroke 28, 1073–1080 (discussion 1080-1071).

Dang, B., Li, H., Xu, X., Shen, H., Wang, Y., Gao, A., He, W., Wang, Z., Chen, G., 2015. Cyclophilin A/cluster of differentiation 147 interactions participate in early brain injury after Subarachnoid Hemorrhage in rats. Crit. Care Med. 43, e369–e381.

Garg, V., Kathiriya, I.S., Barnes, R., Schluterman, M.K., King, I.N., Butler, C.A., Rothrock, C.R., Eapen, R.S., Hirayama-Yamada, K., Joo, K., Matsuoka, R., Cohen, J.C., Srivastava, D., 2003. GATA4 mutations cause human congenital heart defects and reveal an interaction with TBX5. Nature 424, 443–447.

Grilli, M., Goffi, F., Memo, M., Spano, P., 1996. Interleukin-1beta and glutamate activate the NF-kappaB/Rel binding site from the regulatory region of the amyloid precursor protein gene in primary neuronal cultures. J. Biol. Chem. 271, 15002–15007.

Hu, H., Wang, L., Okauchi, M., Keep, R.F., Xi, G., Hua, Y., 2011. Deferoxamine affects heat shock protein expression in heart after intracerebral hemorrhage in aged rats. Acta Neurochir. Suppl. 111, 197–200.

Jia, W., Wu, W., Yang, D., Xiao, C., Huang, M., Long, F., Su, Z., Qin, M., Liu, X., Zhu, Y.Z., 2018. GATA4 regulates angiogenesis and persistence of inflammation in rheumatoid arthritis. Cell Death Dis. 9, 503.

Jiang, J.J., Liu, C.M., Zhang, B.Y., Wang, X.W., Zhang, M., Saijilafu Zhang, S.R., Hall, P., Hu, Y.W., Zhou, F.Q., 2015. MicroRNA-26a supports mammalian axon regeneration in vivo by suppressing GSK3beta expression. Cell Death Dis. 6, e1865.

Jiang, B., Li, L., Chen, Q., Tao, Y., Yang, L., Zhang, B., Zhang, J.H., Feng, H., Chen, Z., Tang, J., Zhu, G., 2017. Role of Glibenclamide in brain injury after intracerebral hemorrhage. Transl. Stroke Res. 8, 183–193.

Kang, C., Xu, Q., Martin, T.D., Li, M.Z., Demaria, M., Aron, L., Lu, T., Yankner, B.A., Campisi, J., Elledge, S.J., 2015. The DNA damage response induces inflammation and senescence by inhibiting autophagy of GATA4. Science 349, aaa5612.

Kato, A., Fukazawa, Y., Ozawa, F., Inokuchi, K., Sugiyama, H., 2003. Activation of ERK cascade promotes accumulation of Vesl-1S/Homer-1a immunoreactivity at synapses. Brain Res. Mol. Brain Res. 118, 33–44.

Klahr, A.C., Dickson, C.T., Colbourne, F., 2015. Seizure activity occurs in the collagenase but not the blood infusion model of striatal hemorrhagic stroke in rats. Transl. Stroke Res. 6, 29–38.

Lan, X., Han, X., Li, Q., Yang, Q.W., Wang, J., 2017. Modulators of microglial activation and polarization after intracerebral haemorrhage. Nat. Rev. Neurol. 13, 420–433.

MacLellan, C.L., Silasi, G., Poon, C.C., Edmundson, C.L., Buist, R., Peeling, J., Colbourne, F., 2008. Intracerebral hemorrhage models in rat: comparing collagenase to blood infusion. J. Cereb. Blood Flow Metab.: official J. Int. Soc. Cereb. Blood Flow Metab 28, 516–525.

Shen, H., Chen, Z., Wang, Y., Gao, A., Li, H., Cui, Y., Zhang, L., Xu, X., Wang, Z., Chen, G., 2015. Role of neurexin-1beta and neuroligin-1 in cognitive dysfunction after subarachnoid hemorrhage in rats. Stroke 46, 2607–2615.

Song, M., Giza, J., Proenca, C.C., Jing, D., Elliott, M., Dincheva, I., Shmelkov, S.V., Kim, J., Schreiner, R., Huang, S.H., Castren, E., Prekeris, R., Hempstead, B.L., Chao, M.V., Dictenberg, J.B., Rafii, S., Chen, Z.Y., Rodriguez-Boulan, E., Lee, F.S., 2015. Slitrk5 mediates BDNF-dependent TrkB receptor trafficking and signaling. Dev. Cell 33, 690–702.

Stefanovic, S., Barnett, P., van Duijvenboden, K., Weber, D., Gessler, M., Christoffels, V.M., 2014. GATA-dependent regulatory switches establish atrioventricular canal specificity during heart development. Nat. Commun. 5, 3680.

Sun, L., Zhang, K., Zhai, W., Li, H., Shen, H., Yu, Z., Chen, G., 2018. TAR DNA binding protein-43 loss of function induced by phosphorylation at s409/410 blocks autophagic flux and participates in secondary brain injury after intracerebral hemorrhage. Front. Cell. Neurosci. 12, 79.

Wang, Y., Gao, A., Xu, X., Dang, B., You, W., Li, H., Yu, Z., Chen, G., 2015. The neuroprotection of lysosomotropic agents in experimental subarachnoid hemorrhage probably involving the apoptosis pathway triggering by cathepsins via chelating Intralysosomal Iron. Mol. Neurobiol. 52, 64–77.

Yamaguchi, M., Zhou, C., Heistad, D.D., Watanabe, Y., Zhang, J.H., 2004. Gene transfer of extracellular superoxide dismutase failed to prevent cerebral vasospasm after experimental subarachnoid hemorrhage. Stroke 35, 2512–2517.

Ye, X., Zuo, D., Yu, L., Zhang, L., Tang, J., Cui, C., Bao, L., Zan, K., Zhang, Z., Yang, X., Chen, H., Tang, H., Zu, J., Shi, H., Cui, G., 2017. ROS/TXNIP pathway contributes to thrombin induced NLRP3 inflammasome activation and cell apoptosis in microglia. Biochem. Biophys. Res. Commun. 485, 499–505.

Yu, W., Huang, X., Tian, X., Zhang, H., He, L., Wang, Y., Nie, Y., Hu, S., Lin, Z., Zhou, B., Pu, W., Lui, K.O., Zhou, B., 2016. GATA4 regulates Fgf16 to promote heart repair after injury. Development 143, 936–949.

Zhai, W., Chen, D., Shen, H., Chen, Z., Li, H., Yu, Z., Chen, G., 2016. A1 adenosine receptor attenuates intracerebral hemorrhage-induced secondary brain injury in rats by activating the P38-MAPKAP2-Hsp27 pathway. Mol. Brain 9, 66.

Zhang, J.S., Herreros-Villanueva, M., Koenig, A., Deng, Z., de Narvajas, A.A., Gomez, T.S., Meng, X., Bujanda, L., Ellenrieder, V., Li, X.K., Kaufmann, S.H., Billadeau, D.D., 2014. Differential activity of GSK-3 isoforms regulates NF-kappaB and TRAIL- or TNFalpha induced apoptosis in pancreatic cancer cells. Cell Death Dis. 5, e1142.